The high expression of immune checkpoint co-stimulators predicts a favorable prognosis in head and neck carcinomas

Shi-Rou Chang
National Yang Ming Chiao Tung University
Chung-Hsien Chou
National Yang Ming Chiao Tung University
Hsi-Feng Tu
National Yang Ming Chiao Tung University
Chung-Ji Liu
National Yang Ming Chiao Tung University
Kuo-Wei Chang
ckcw@ym.edu.tw
National Yang Ming Chiao Tung University
Shu-Chun Lin
National Yang Ming Chiao Tung University

Research Article

Keywords: CD27, CD30, CD40L, ICOS, OX40, head and neck cancer; oral cancer

Posted Date: March 14th, 2024

DOI: https://doi.org/10.21203/rs.3.rs-3995490/v1

Additional Declarations: No competing interests reported.

The high expression of immune checkpoint co-stimulators predicts a favorable prognosis in head and neck carcinomas

Shi-Rou Chang[1], Chung-Hsien Chou[1], Hsi-Feng Tu[1,2], Chung-Ji Liu[2,3], Kuo-Wei Chang[1,2,4*], Shu-Chun Lin[1,2,4*]

[1]Institute of Oral Biology, [2]Department of Dentistry, College of Dentistry, National Yang Ming Chiao Tung University, Taipei, Taiwan.
[3]Department of Dentistry, Taipei Mackay Memorial Hospital, Taipei, Taiwan
[4]Department of Stomatology, Taipei Veterans General Hospital, Taipei, Taiwan

[*]Correspondence: shuchun@nycu.edu.tw; ckcw@nycu.edu.tw

Short title: Immune checkpoint co-stimulators in HNSCC

Keywords: CD27, CD30, CD40L, ICOS, OX40, head and neck cancer; oral cancer

Declarations

Ethics Approval and Consent to Participate: Nil

Consent for publication

The authors consent to the publication of this work.

Availability of data and material

The datasets used and/or analyzed during the current study are available from the corresponding author upon reasonable request.

Competing interest

The authors declare that they have no competing interests.

Funding

This study was supported by grants 108-2314-B-010-010-MY3 and NSTC 112-2314-B-A49-006 from the National Science and Technology Council (NSTC), Taiwan.

Authors' contribution

Conception/Design: CSR, CKW and LSC

Collection and assembly of data: CSR, CCH, THF and LCJ

Data analysis and interpretation: CSR, CCH, THF, CKW and LSC

Manuscript writing: CSR, CKW and LSC

All authors read and approved the final manuscript.

Correspondence:

Shu-Chun Lin PhD Professor Institute of Oral Biology College of Dentistry National Yang Ming Chiao Tung University Taipei, Taiwan e-mail: shuchun@nycu.edu.tw fax: +8862-28264053	Kuo-Wei Chang DDS, PhD Professor Department of Dentistry College of Dentistry National Yang Ming Chiao Tung University Taipei, Taiwan e-mail: ckcw@nycu.edu.tw fax: +886228264053

Abstract

Objectives: T cells require second immune checkpoint molecules for activation and immune memory after antigen presentation. In our previous study, we found ICOS a favorable prognostic factor amongst B7 immune checkpoint co-stimulators (ICSs) families in head and neck squamous cell carcinoma (HNSCC) and oral SCC (OSCC).

Materials and method: This study analyzed the expression of on-B7 TNF ligand/receptor superfamily ICSs in the Cancer Genome Atlas (TCGA) HNSCC cohort, our OSCC cohort, and pan-cancer datasets. The correlation in expression, prognosis, and immune status was assessed.

Results: The higher expression of CD27, CD30, CD40L, DR3, and OX40, presumably on the T cell surface, defined better overall survival of HNSCC patients. Besides, CD27, CD30, CD40L, and OX40 were highly correlated with ICOS expression in tumors. CD27, CD40L, and DR3 expression are higher in HPV+ HNSCC tumors than in HPV- tumors. The combined expression level of CD27/OX40 or CD27/CD40L/OX40 enables the potent survival prediction of small, less nodal involvement, early stage, and HPV+ tumor subsets. In both HNSCC and our OSCC cohorts, tumors expressing high CD27, CD30, CD40L, ICOS, and OX40 exhibited enhanced immune cell infiltration. The high correlation in the expression of these ICSs is also noted in the vast majority of tumor types in addition to HNSCC in TCGA datasets.

Conclusion: The findings suggest that the concordant stimulation of CD27, CD30, CD40L, ICOS, and OX40 could be a crucial strategy in cancer immunotherapy.

Abstract

Following antigen presentation, T cells require second immune checkpoint molecules for activation and immune memory. In our previous study, we found ICOS a favorable prognostic factor amongst B7 immune checkpoint co-stimulators (ICCs) families in head and neck squamous cell carcinoma (HNSCC) and oral SCC (OSCC). This study further identifies the frequent upregulation of expression in the non-B7 TNF ligand/receptor superfamily ICCs in the Cancer Genome Atlas (TCGA) HNSCC dataset. The higher expression of CD27, CD30, CD40L, DR3, and OX40, presumably on the T cell surface, defined better overall survival of HNSCC patients. Besides, CD27, CD30, CD40L, and OX40 were highly correlated with ICOS expression in tumors. CD27, CD40L, and DR3 expression are higher in HPV+ HNSCC tumors than in HPV- tumors. The combined expression level of CD27/OX40 or CD27/CD40L/OX40 enables the potent survival prediction of small, less nodal involvement, early stage, and HPV+ tumor subsets. In both HNSCC and our OSCC cohorts, tumors expressing high CD27, CD30, CD40L, ICOS, and OX40 exhibited enhanced immune cell infiltration. As high correlation in the expression of these ICSs is also noted in the vast majority of tumor types in addition to HNSCC in TCGA datasets, our findings suggest the concordant stimulation of CD27, CD30, CD40L, ICOS, and OX40 could be a crucial strategy in cancer immunotherapy.

Objectives

Head and neck squamous cell carcinoma (HNSCC), including oral SCC (OSCC), is one of the leading causes of cancer death worldwide. Despite advances in therapies, the 5-year survival rate of HNSCC/OSCC patients remains around 50% over the past decades. The prognosis of HNSCC, especially advanced-stage tumors, remains poor because of the resistance to therapy, relapse, and distal metastasis. Therapeutic targeting of immune components in tumor microenvironment (TIME) is a modern therapeutic modality against malignancies [1]. Immune checkpoint blockade (ICB) drugs, especially those on PD-1, have achieved marked progress in tumor interception, including the therapies against HNSCC [2-5]. However, delineating the immune checkpoint signature and the tumor-infiltrating lymphocytes (TILs) profile in TIME and defining their clinical implication would validate more effective tumor targeting to improve patient outcomes [6, 7].

Following antigen presentation, T cells require second immune checkpoint molecules (ICMs), including immune co-stimulatory (ICS) or immune co-inhibitory signals for activation and immune memory. ICMs consist of B7 and non-B7 subgroups. Among 12 B7 ICM members, we have elucidated that ICOS is the most crucial prognostic predictor in our cohort's TCGA HNSCC dataset and OSCC [8, 9]. Non-B7 ICS family comprising at least seven paired tumor necrosis factor (TNF) family ligand/receptor complexes including 4-1BB (CD137), CD27, CD30, CD40L, death domain 3 (DR3), glucocorticoid-induced TNFR-related receptor (GITR) and OX40 (CD134) on the T-cell and their coupled 4-BBL, CD70, CD30L, CD40, TNF-family ligand (TL1A), GITRL and OX40L on the antigen-presenting cells, other immune cell types or tumor cell surface [10]. ICSs have garnered significant attention recently for mechanistic approaches or being designed as co-targeting to facilitate tumor immunity [10, 11].

Aberrant 4-1BB (CD137) expression has been found on TIL and peripheral blood lymphocyte (PBL) of HNSCC patients [11-13]. CD27/CD70 (CD27 ligand) complex transduces signals leading to NFκB and JNK activation, which regulate B-cell activation and immunoglobulin synthesis [14]. CD27/CD70 appeared to be the diagnostic markers or survival predictors of HNSCC [15, 16], and CD27 agonists could be adjuvant to anti-PD1 therapy [17]. Chimeric antigen receptor (CAR)-T cell targeting CD70 has been developed to intercept HNSCC [18]. Likewise, CD30 also contributes to the activation of NFκB and MAPK, which results in pro-survival effects [19]. It is a marker of activated lymphocytes highly expressed in hematopoietic malignancies being tested as a CAR-T therapeutic target in refractory lymphomas [20, 21]. However, the expression profile of CD30/CD30L in HNSCC has been hitherto undefined. The gradual decrease of CD40 expression in monocytes and CD40L expression in T cells was noted during HNSCC progression [6, 22]. The antitumor effect on the CD40 expression was associated with the cytokine production. The signals of TL1A functioning through DR3 are a target of TNFα, which drives pluripotential activities in immunity and tumor pathogenesis [23-25]. GITR is upregulated in TIL and T cell subsets of PBL in HNSCC patients relative to normal controls [13]. The expression of OX40 (CD134) is primarily expressed on activated T cells, and it mediates memory, anti-apoptosis, proliferation, and survival [26, 27]. OX40+ T cells are found in

various solid malignancies and are prevalent in HNSCC [13, 26, 27]. Due to the tumor suppressive activity, clinical trials of OX40-directed immune stimulation therapy against HNSCC are undergoing [5, 26, 28].

Although blockage of immune inhibitors rendered remarkable progress in cancer therapy [4], precision targeting has unmet needs to improve patient outcomes. This study provides a comprehensive insight into immune stimulators in the TIME of HNSCC to facilitate immunotherapy. The profiling of the ICS landscape identified that CD27, CD30, CD40L, DR3, ICOS, and OX40 were determinants of HNSCC patient survival. These ICSs could be clinical markers or promising co-targets for HNSCC therapy.

Materials and Methods

HNSCC transcriptional signatures

Patient information for HNSCC and normal tissue information was retrieved from The Cancer Genome Atlas (TCGA, https://portal.gdc.cancer.gov/). Hereon defined as TCGA HNSCC cohort. The expression matrix of genes based on the fragments per kilobase of transcript per million mapped reads (FPKM) format normalizing samples was used for cross-comparison.

OSCC transcriptional signatures

RNA-Seq data from 54 OSCC patients and 28 matched normal tissues of our cohort were established previously [8]. The cohort characteristics were described in our previous study. Transcripts per kilobase of transcript per million (TPM) mapped reads designated the clean reads of RNA-Seq.

Cell culture, induction of isografts, and RNA-Seq

Murine OSCC cell line MTCQ1 was cultivated as previously described [29]. Inoculation of MTCQ1 isografts into the buccal space of C57BL/6J mice (National Laboratory Animal Center, Taipei, Taiwan) was performed [30]. After sacrificing animals, the grafts and the adjacent buccal mucosa were resected, processed, and subjected to RNA-Seq. The expression matrix of genes shown as TPM values was subjected to analysis. The animal study was approved by the Institutional Animal Care and Use Committee (IACUC) of National Yang Ming University (IACUC approval no.: 1080602).

Pan-cancer transcriptional signatures

The pan-cancer profile in the TCGA database, including 32 cancer studies, was achieved from the TIMER dataset (https://cistrome.shinyapps.io/timer/) or the ENCORI portal (https://rnasysu.com/encori/). Bubble plots and heatmaps designated the differences across settings.

Bioinformatic analysis

Immunization-related information, tumor-infiltrating immune cells, and variable cellular contexts were analyzed using EPIC (E), MCPCOUNT (M), QUANTISEQ (Q), TIMER (T), and XCELL (X) modes [31]. Heatmaps illustrated the differential landscape across settings.

Statistics

Data were presented as mean ± standard error (SE) or other formats. Mann-Whitney test, *t*-test, and correlation analysis were performed. Kaplan-Meier survival analysis was used to assess the overall survival (OS). The prediction accuracy of the patient survival was evaluated by time-dependent receiver operating characteristic curve (ROC) mode. The prognostic signatures were also analyzed using a multivariate Cox regression module and illustrated using Lollipop plots.

Results

1. Dysregulation of non-B7/CD28 ICS in HNSCC and OSCC

Analysis of 7 paired non-B7/CD28 ICS ligand-receptor complex molecules, including 4-1BB/4-1BBL, CD27/CD70, CD30/CD30L, CD40L/CD40, DR3/TL1A, GITR/GITRL, and OX40/OX40L was carried out in 44 normal tissue and 502 HNSCC tumors from the TCGA HNSCC cohort. It revealed the upregulation of 4-1BB, CD27, CD30, DR3, GITR, and OX40 expression and the downregulation of CD40L expression, presumably expressed in the immune cell fraction of tumor tissues compared to normal counterparts. In addition, the coupled 4-1BBL, CD70, CD40, and OX40L, presumably expressed in tumor cell or APC fraction, was also upregulated in tumors (Fig. 1A). The co-upregulation of 4-1BB/4-1BBL, downregulation of CD40L/upregulation of CD40, upregulation of CD70 and OX40L, and the downregulation of TL1A being identified in our OSCC cohort was in agreement with findings in TCGA HNSCC cohort (Fig. 1B). Among 89 HNSCC examined with in situ hybridization, 22 (24.7%) are HPV positive. The HPV+ tumors exhibit a better survival relative to HPV- cases (not shown). Of note, the expression of CD27, CD40L, and DR3 was higher in HPV+ HNSCC in relation to HPV- HNSCC (Fig. 1C). Except for CD40L, the expression of most ICSs was also higher in the murine isografic MTCQ1 tumors than control oral mucosa (Fig. 1D). The general upregulation of ICSs was seen in TCGA HNSCC tumors, human OSCC and murine OSCC isografts.

2. Association of higher CD27, CD30, CD40L, DR3, ICOS, and OX40 expression with better HNSCC survival

The higher expression of CD27, CD30, CD40L, DR3, OX40, and ICOS, presumably localized on the T cell surface, defined the better overall survival of HNSCC tumors in Kaplan-Meier plots, with hazard ratios 0.61, 0.40, 0.50, 0.68, 0.63 and 0.67, respectively (Fig. 2A, B). The expression of other non-B7 ICSs was not associated with HNSCC survival. The expression of ICSs was also the prognostic predictor of other malignancies in the TCGA dataset, either for favorable or unfavorable prognosis. Nevertheless, the prediction power of these ICSs in HNSCC stands on the leading rank in the malignancies exhibiting favorable prognosis (Fig. 2B). Multivariate logistic regression specified the expression level of each molecule as an independent prognostic predictor of HNSCC (Fig. 2B). CD27 was the best solitary independent prognostic predictor of HNSCC. Besides, the higher ICOS expression in HPV+ HNSCC defined a worse prognosis (Fig. 2D). Since there was remarkable inter-correlation across the expression of CD27, CD30, CD40L, ICOS, and OX40 across HNSCC and

OSCC. However, no consistent correlation between DR3 and other ICSs was found (Fig. 2E), and DR3 was excluded in the subsequent analysis.

3. Combined ICS analysis enables more powerful prognostic prediction of HNSCC subsets

Multivariate logistic regression specified the combined expression level of ICSs, except for one combination, as independent prognostic predictors of overall survival in HNSCC (Fig. 3A, Table S1). Moreover, the ROC analysis of one-year to three-year follow-up confirmed that the discrimination power of the combined ICSs analysis was time-dependent (Fig. 3B). Moreover, the combination of OX40 or CD40L/OX40 increased the prediction power of CD27 in the survival of T1,2, N0, 1 and HPV+ rumor subsets (Fig. 3C). Representative analyses are shown in Fig. 4D. The CD27, CD40L, and ICOS expressions were associated with differentiation grade in both HNSCC and OSCC cohorts. However, the association trend appeared diverse between them (Fig. S1).

4. Homogenous ICS expression is present within major human malignant tumors

The diverse landscape of CD27, CD30, CD40L, ICOS, and OX40 expression between major cancers, including breast invasive carcinoma (BRCA), colorectal adenocarcinoma (COAD), lung adenocarcinoma (LUAD), lung squamous cell carcinoma (LUSC), and glioblastoma (GBM), and their paired normal tissues in the TCGA database was notified (Fig. 4A). Except for COAD, CD27 expression in tumors was high in tumors. Unlike HNSCC, CD30 was downregulated in most major malignancies. Like HNSCC, CD40L was downregulated, and OX40 was upregulated in most malignancies. The expression states of CD40L, ICOS, and OX40 were relatively homogeneous in major malignancies (Fig. 4B). The expression of ICSs in GBM was generally lower than in other tumors.

5. Immerse inter-correlation across CD27, CD30, CD40L, ICOS, and OX40 expression is notified in pan-cancers

Despite the variation in expression, the inter-correlation of each two of the dysregulated ICSs was extremely high amongst tumors as in 88% (282/320) of comparison pairs; the correlation was highly significant. (Fig. 5A, Table S2 - Table S11). In 53% (17/32) types of malignancies, the expression of all these five molecules was highly correlated. Fig. 5B shows the *r* values in major malignancies. The correlation of ICSs in BRCA and LUSC was extremely high. The high correlation between CD27 and ICOS and between CD40L and ICOS was noticed in all types of malignancies (Fig. 5A, B). However, such inter-correlation in immune cell malignancies, including diffuse large B cell lymphoma (DLBC) and acute myeloid leukemia (LAML), was much weaker than non-immune malignancies.

6. The immune profile is associated with ICS expression in tumors

Bioinformatic algorithms revealed a substantially positive correlation between ICS expression level and immune scores, especially lymphocyte infiltration, including B cells, CD8+ T cells, macrophage,

MDSC, and neutrophil in both HNSCC and OSCC tumor cohorts (Fig. 6A). High CD27, CD40L, and ICOS expression were particularly highly associated with TIL scores (Fig. 6A, B). The association between these molecules with stromal or endothelial cells was inconsistent across cohorts. These ICS molecules seemed negatively associated with other cells, mostly un-characterized or tumor cells.

Conclusions

HNSCC/OSCC exhibits multifaceted abnormalities and poses significant therapeutic challenges, with only a limited number of drugs demonstrating efficacy against this disease. Multiple immunotherapy strategies, including ICB drugs, co-stimulatory agonists, antigenic vaccines, adoptive T cell transfer, oncolytic virus therapy, and others, have been proposed to intercept malignancies [5]. The profiling of ICM and TIL cell subsets in tumors would render the selection of appropriate targeting strategies. This study identifies the concordant upregulation of six of seven non-B7 ICSs in the TIL of HNSCC, albeit CD40L is downregulated. Besides, the upregulation of 4-1BB, CD27, and OX4 in TIL co-exists with the upregulation of matched 4-1BBL, CD70, and OX40L on tumor cells. Previous reports have only signified the co-upregulation of CD27/CD70 in HNSCC [15, 16]. The co-upregulation of 4-1BB/4-1BBL and OX40/OX40L newly found in this study may denote their roles in tumor immune activation. Although the analytical power of our OSCC cohort is lower than the TCGA HNSCC sample cohort, probably owing to the sample size limitation, the expression profile of ICSs in OSCC is similar to that in HNSCC. Likewise, although the analytical strength of orthotopic syngeneic murine tumors is impeded by analyzing multiple grafts derived from the same cell line, the trend of ICM change in the mouse OSCC model simulates that of human HNSCC [29]. The findings confirm the eminent and concordant dysregulation of non-B7 ICS members in HNSCC. As eminent metastasis can be perceived in this model, the association between immune disruption and metastatic progression could be addressed using this model [29, 32].

We found that the higher expression of CD27, CD30, CD40L, DR3, ICOS, and OX40 is associated with better patient survival in HNSCC. The high expression of these ICSs in tumors predisposes to a favorable rather than unfavorable prognosis. CD27 exhibits the most potent prediction power in HNSCC, next by OX40, CD40L, and ICOS. As the prediction power of CD27, CD40L, ICOS, and OX40 in HNSCC ranks in the leading edge among all malignancies, together with their high intercorrelation in expression, these ICSs could be considered HNSCC-specific prognosticators. Studies have revealed elevated expression levels of CD27 in HNSCC tumors compared to normal tissues, suggesting its pathogenetic implications. As higher expression of CD27 in HNSCC tumors has been associated with improved survival outcomes, the administration of CD27 agonists has been suggested by previous research as a feasible strategy for HNSCC interception [17]. This approach also suggests that strategies aiming at modulating CD27 signaling may be explored as part of immunotherapeutic interventions once the findings are ascertained by protein-based analysis. The roles of CD70 as a partner of CD27 also require specification [7]. ICOS has been an active immune response and better patient survival in HNSCC/OSCC tumors [8]. Another known effect is the prevalence of

OX40+ T cells in HNSCC [13, 26, 27], which leads to potential OX40-directed immune stimulation therapy against HNSCC [26, 28]. CD40L is one of the favorable prognostic predictors of HNSCC [6]. Our stratification highlights the enrichment of prognostic values in small, early-stage, less metastatic, and HPV+ HNSCC subsets by combining these predictors with CD27. This comprehensive study provides additional clues substantiating that the co-upregulation of CD27, CD40L, ICOS, and OX40 could be essential targets in HNSCC immunotherapy. Although the diverse expression landscape across tumors underscores the need for tailored therapeutic approaches, simultaneous targeting of these co-stimulatory pathways may enhance the efficacy of immunotherapeutic interventions.

Since the concordance in the expression of CD27, CD30, CD40L, ICOS, and OX40 are eminent in HNSCC, we extended the expression analysis to a broad spectrum of malignancies. Although the expression levels of ICSs are divergent across major malignancies of the breast, colon, and lung when compared to their normal controls, the expression profiles of CD27, CD40L, and ICOS within the same type of tumor are generously homogenous, which may suggest the co-activation of these ICSs in these pivotal human cancers. The diverse expression in some types of normal tissue due to various degrees of inflammatory cellular infiltration or the paucity of samples may also complicate the differences in expression across normal and tumor tissues. Alongside HNSCC, CD40L downregulation and OX40 upregulation are common in these major malignancies. Pan-cancer analysis further reveals the high inter-correlation of ICSs in most malignancies. The high inter-correlation amongst CD27/CD40L/ICOS, especially the correlation between CD40L and ICOS, existing in nearly all tumors, may suggest the co-targeting values in global cancer therapy. The discrepancies between immune and non-immune solid malignancies highlight the unique characteristics of immune-related interactions in TIME. The findings in pan-cancer also suggest the existence of potential synergistic interaction or shared regulatory mechanisms, underscoring the complexity of immune checkpoint networks in cancers [5].

Compatible with favorable survival found in HNSCC patients with high ICS expression, the tumor immune score also correlates with ICS expression. The observed correlation with TIL further emphasizes the role of ICSs in the TIME. Recent advances in ICB have shed light on managing complex cases, while the combined co-stimulation of ICSs for TIL enrichment could be a potential adjuvant strategy [4, 5]. The comprehensive analysis of the ICS profile would contribute valuable insights for developing targeted therapies and personalized treatment strategies for HNSCC.

Conclusion

This study delineates the prognostic significance of CD27, CD30, CD40L, ICOS, and OX40 expression in HNSCC, with CD27 demonstrating potent predictive power. The combined assessment of these molecules provides valuable insights into risk stratification and prognosis for HNSCC patients.

Acknowledgments

This study was supported by grants 108-2314-B-010-010-MY3 and NSTC 112-2314-B-A49-006 from the National Science and Technology Council (NSTC), Taiwan.

References

[1] Ulevitch RJ. Therapeutics targeting the innate immune system. Nat Rev Immunol. 2004;4:512-20.
[2] Masarwy R, Kampel L, Horowitz G, Gutfeld O, Muhanna N. Neoadjuvant PD-1/PD-L1 Inhibitors for Resectable Head and Neck Cancer: A Systematic Review and Meta-analysis. JAMA Otolaryngol Head Neck Surg. 2021;147:871-8.
[3] van der Leun AM, Traets JJH, Vos JL, Elbers JBW, Patiwael S, Qiao X, et al. Dual Immune Checkpoint Blockade Induces Analogous Alterations in the Dysfunctional CD8+ T-cell and Activated Treg Compartment. Cancer Discov. 2023;13:2212-27.
[4] Miyashita H, Kurzrock R, Bevins NJ, Thangathurai K, Lee S, Pabla S, et al. T-cell priming transcriptomic markers: implications of immunome heterogeneity for precision immunotherapy. NPJ Genom Med. 2023;8:19.
[5] Sun Q, Hong Z, Zhang C, Wang L, Han Z, Ma D. Immune checkpoint therapy for solid tumors: clinical dilemmas and future trends. Signal Transduct Target Ther. 2023;8:320.
[6] Baysal H, Siozopoulou V, Zaryouh H, Hermans C, Lau HW, Lambrechts H, et al. The prognostic impact of the immune signature in head and neck squamous cell carcinoma. Front Immunol. 2022;13:1001161.
[7] Nilsson MB, Yang Y, Heeke S, Patel SA, Poteete A, Udagawa H, et al. CD70 is a therapeutic target upregulated in EMT-associated EGFR tyrosine kinase inhibitor resistance. Cancer Cell. 2023;41:340-55 e6.
[8] Chang SR, Chou CH, Liu CJ, Lin YC, Tu HF, Chang KW, et al. The Concordant Disruption of B7/CD28 Immune Regulators Predicts the Prognosis of Oral Carcinomas. Int J Mol Sci. 2023;24.
[9] Zhao X, Wang Y, Jiang X, Mo B, Wang C, Tang M, et al. Comprehensive analysis of the role of ICOS (CD278) in pan-cancer prognosis and immunotherapy. BMC Cancer. 2023;23:194.
[10] Sadeghirad H, Liu N, Monkman J, Ma N, Cheikh BB, Jhaveri N, et al. Compartmentalized spatial profiling of the tumor microenvironment in head and neck squamous cell carcinoma identifies immune checkpoint molecules and tumor necrosis factor receptor superfamily members as biomarkers of response to immunotherapy. Front Immunol. 2023;14:1135489.
[11] Economopoulou P, Kotsantis I, Psyrri A. The promise of immunotherapy in head and neck squamous cell carcinoma: combinatorial immunotherapy approaches. ESMO Open. 2016;1:e000122.
[12] Bin-Alee F, Chunthagonesupawit N, Meesakul T, Diloktaweewattana A, Mahattanasakul P, Mutirangura A, et al. High 4-1BB Expression in PBMCs and Tumor Infiltrating Lymphocytes (TILs) in Patients with Head and Neck Squamous Cell Carcinoma. Eur J Dent. 2023.
[13] Puntigam LK, Jeske SS, Gotz M, Greiner J, Laban S, Theodoraki MN, et al. Immune Checkpoint Expression on Immune Cells of HNSCC Patients and Modulation by Chemo- and

Immunotherapy. Int J Mol Sci. 2020;21.
[14] Takeuchi T, Tsuzaka K, Kameda H, Amano K. Therapeutic targets of misguided T cells in systemic lupus erythematosus. Curr Drug Targets Inflamm Allergy. 2005;4:295-8.
[15] De Meulenaere A, Vermassen T, Aspeslagh S, Zwaenepoel K, Deron P, Duprez F, et al. CD70 Expression and Its Correlation with Clinicopathological Variables in Squamous Cell Carcinoma of the Head and Neck. Pathobiology. 2016;83:327-33.
[16] Wang F, Zhang W, Chai Y, Wang H, Liu Z, He Y. Constrast-enhanced computed tomography radiomics predicts CD27 expression and clinical prognosis in head and neck squamous cell carcinoma. Front Immunol. 2022;13:1015436.
[17] Sanborn RE, Pishvaian MJ, Callahan MK, Weise A, Sikic BI, Rahma O, et al. Safety, tolerability and efficacy of agonist anti-CD27 antibody (varlilumab) administered in combination with anti-PD-1 (nivolumab) in advanced solid tumors. J Immunother Cancer. 2022;10.
[18] Park YP, Jin L, Bennett KB, Wang D, Fredenburg KM, Tseng JE, et al. CD70 as a target for chimeric antigen receptor T cells in head and neck squamous cell carcinoma. Oral Oncol. 2018;78:145-50.
[19] van der Weyden CA, Pileri SA, Feldman AL, Whisstock J, Prince HM. Understanding CD30 biology and therapeutic targeting: a historical perspective providing insight into future directions. Blood Cancer J. 2017;7:e603.
[20] Fu Z, Li S, Han S, Shi C, Zhang Y. Antibody drug conjugate: the "biological missile" for targeted cancer therapy. Signal Transduct Target Ther. 2022;7:93.
[21] Ramos CA, Grover NS, Beaven AW, Lulla PD, Wu MF, Ivanova A, et al. Anti-CD30 CAR-T Cell Therapy in Relapsed and Refractory Hodgkin Lymphoma. J Clin Oncol. 2020;38:3794-804.
[22] Sathawane D, Kharat RS, Halder S, Roy S, Swami R, Patel R, et al. Monocyte CD40 expression in head and neck squamous cell carcinoma (HNSCC). Hum Immunol. 2013;74:1-5.
[23] Zhang D, Yang H, Dong XL, Zhang JT, Liu XF, Pan Y, et al. TL1A/DR3 Axis, A Key Target of TNF-a, Augments the Epithelial-Mesenchymal Transformation of Epithelial Cells in OVA-Induced Asthma. Front Immunol. 2022;13:854995.
[24] Valatas V, Kolios G, Bamias G. TL1A (TNFSF15) and DR3 (TNFRSF25): A Co-stimulatory System of Cytokines With Diverse Functions in Gut Mucosal Immunity. Front Immunol. 2019;10:583.
[25] Richard AC, Tan C, Hawley ET, Gomez-Rodriguez J, Goswami R, Yang XP, et al. The TNF-family ligand TL1A and its receptor DR3 promote T cell-mediated allergic immunopathology by enhancing differentiation and pathogenicity of IL-9-producing T cells. J Immunol. 2015;194:3567-82.
[26] Bell RB, Leidner RS, Crittenden MR, Curti BD, Feng Z, Montler R, et al. OX40 signaling in head and neck squamous cell carcinoma: Overcoming immunosuppression in the tumor microenvironment. Oral Oncol. 2016;52:1-10.
[27] Alves Costa Silva C, Facchinetti F, Routy B, Derosa L. New pathways in immune stimulation:

targeting OX40. ESMO Open. 2020;5.
[28] Duhen R, Ballesteros-Merino C, Frye AK, Tran E, Rajamanickam V, Chang SC, et al. Neoadjuvant anti-OX40 (MEDI6469) therapy in patients with head and neck squamous cell carcinoma activates and expands antigen-specific tumor-infiltrating T cells. Nat Commun. 2021;12:1047.
[29] Chen YF, Chang KW, Yang IT, Tu HF, Lin SC. Establishment of syngeneic murine model for oral cancer therapy. Oral Oncol. 2019;95:194-201.
[30] Lu YJ, Deng YT, Ko HH, Peng HH, Lee HC, Kuo MY, et al. Lysyl oxidase-like 2 promotes stemness and enhances antitumor effects of gefitinib in head and neck cancer via IFIT1 and IFIT3. Cancer Sci. 2023;114:3957-71.
[31] Chi H, Yang J, Peng G, Zhang J, Song G, Xie X, et al. Circadian rhythm-related genes index: A predictor for HNSCC prognosis, immunotherapy efficacy, and chemosensitivity. Front Immunol. 2023;14:1091218.
[32] Chen HH, Yu HI, Rudy R, Lim SL, Chen YF, Wu SH, et al. DDX3 modulates the tumor microenvironment via its role in endoplasmic reticulum-associated translation. iScience. 2021;24:103086.

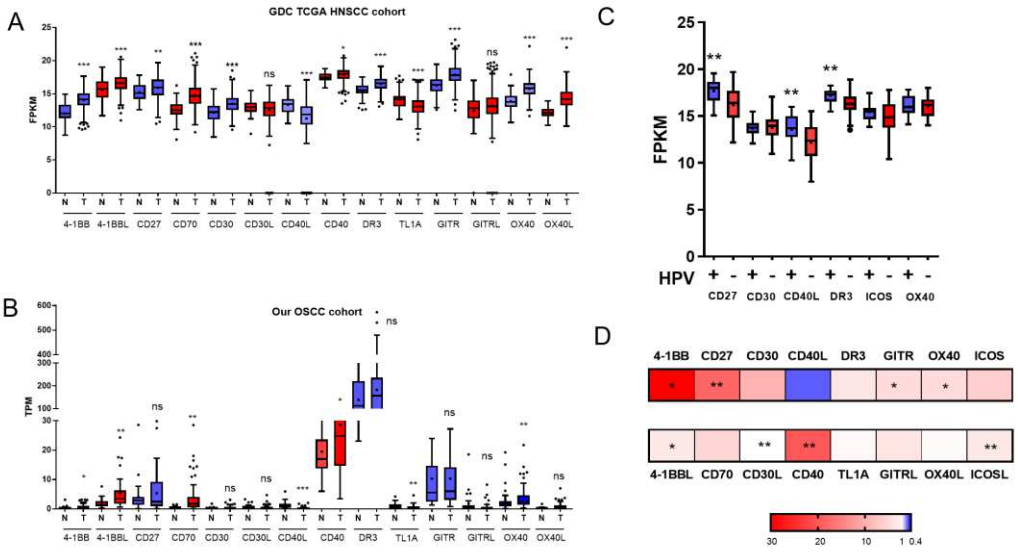

Fig. 1. Transcriptomic profiles of 14 ICSs. (A - C) Box and Whiskers plots. (A) TCGA HNSCC tumors. (B) our OSCC cohort. (C) TCGA HNSCC tumors are characterized to be HPV+ or HPV-. N is normal tissue; T is tumor tissue. +, medium value. Y-axis in HNSCC, FPKM; Y-axis in OSCC, TPM. (D) Heatmap to illustrate the ratio of mean TPM in 6 individual MTCQ1 buccal isografts/mean TPM in 3 individual buccal mucosa tissues. *ns*, not significant. *, ** and *** represent $p < 0.05$, $p < 0.01$ and $p < 0.001$, respectively. *t*-test or Mann-Whitney test.

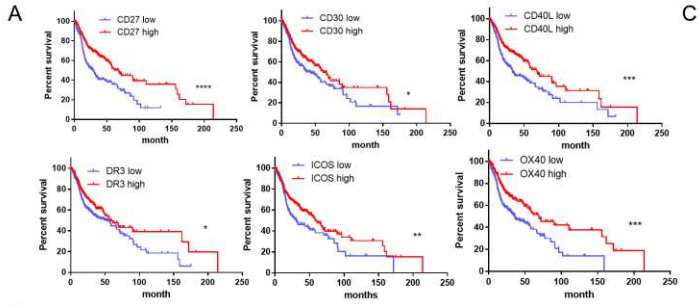

B

CD27		CD30		CD40L		DR3		ICOS		OX40	
HR	*p*	HR	*p*	HR	*p*	HR	*p*	HR	*p*	HR	*p*
0.52	<0.0001	0.77	0.011	0.61	0.0003	0.74	0.005	0.67	0.003	0.58	0.0002

C

	Favorable: Unfavorable (cancer types)	Favorable ranking (*p*)
CD27	6: 1	1/6
CD30	6: 1	6/6
CD40L	8: 2	1/8
DR3	5: 2	2/5
ICOS	11: 2	4/11
OX40	3: 4	1/3

D

	CD27		CD30		CD40L		DR3		ICOS		OX40	
	HR	*p*	HR	*p*	HR	*p*	HR	*p*	HR	*p*	HR	*p*
HPV+	0.19	0.11	0.61	0.26	0.80	0.41	1.54	0.69	2.15	0.04	3.88	0.68
HPV-	0.34	0.26	0.80	0.67	0.57	0.72	2.33	0.18	3.09	0.60	1.49	0.87

E

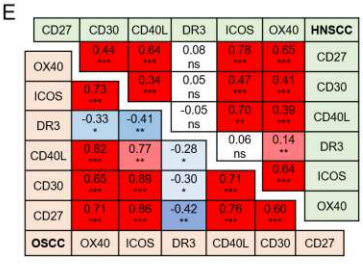

Fig. 2. The implications of CD27, CD30, CD40L, DR3, ICOS and OX40 expression. (A - C) Survival analysis. (A) Kaplan-Meier curve analysis of these ICSs in HNSCC tumors. (B) The hazard ratio and *p* value are related to each ICS in (A). (C) The states of these ICSs in malignancies. Lt column shows the states of high expression of these ICSs as favorable or unfavorable prognostic markers. Numbers, the number of cancer types. The Rt column shows the rank of *p* values of these ICSs in HNSCC as related to those in all favorable tumors. (D) The survival analysis of these ICSs according to HPV states. (E) Heatmap illustrating the inter-correlation in the expression of these ICSs in HNSCC and

OSCC. Numbers, *r* value; stars, *p* values. *ns*, not significant. *, **, *** and **** represent $p < 0.05$, $p < 0.01$, $p < 0.001$, $p < 0.0001$, respectively. Correlation analysis.

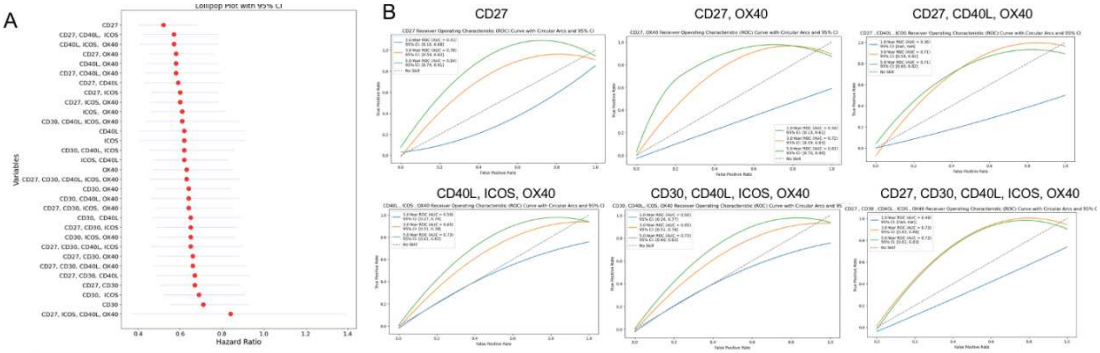

C

KM	CD27	CD27, OX40	CD27, CD40L, OX40	CD40L, ICOS, OX40	CD30, CD40L, ICOS, OX40	CD27, CD30, CD40L, ICOS, OX40
T1, 2	**	****	***	***	**	***
T3, 4	**	*	***	ns	ns	ns
N0, 1	ns	****	***	**	ns	**
N2, 3	**	*	*	ns	ns	ns
Stage I, II	*	**	**	**	*	*
Stage III, IV	****	*	***	**	**	***
HPV+	ns	**	*	**	*	*
HPV-	ns	ns	ns	ns	ns	ns

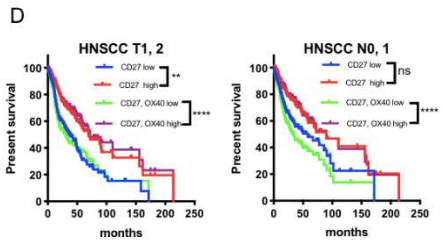

Fig. 3. The prognostic implications of the combined analysis of CD27, CD30, CD40L, ICOS, and OX40 expression. (A) Lollipop plots to illustrate the hazard ratios (dots) and 95% confidence interval of 28 combined groups derived from a multivariate module. The risk scores are achieved from each combination's regression coefficients and expression level. The groups labeled with stars are subjected to analysis in (B, C). (B) Year-dependent ROC analysis of OS. Blue curve, one year; red curve, three-year; green curve, five-year. A year-dependent increase of AUC is notified in most analyzed groups. (C, D) Kaplan-Meier survival analysis. (C) Analysis of tumor subgroups using the medium values of risk scores of patients. (D) Representative analysis to compare the dissection power of CD27 *vs* CD27/OX40 in N0, 1 patient subgroup (Lt panel) and stage I, II patient subgroup (Rt panel). *ns*, not significant. *, **, *** and **** represent $p < 0.05$, $p < 0.01$, $p < 0.001$, $p < 0.0001$, respectively.

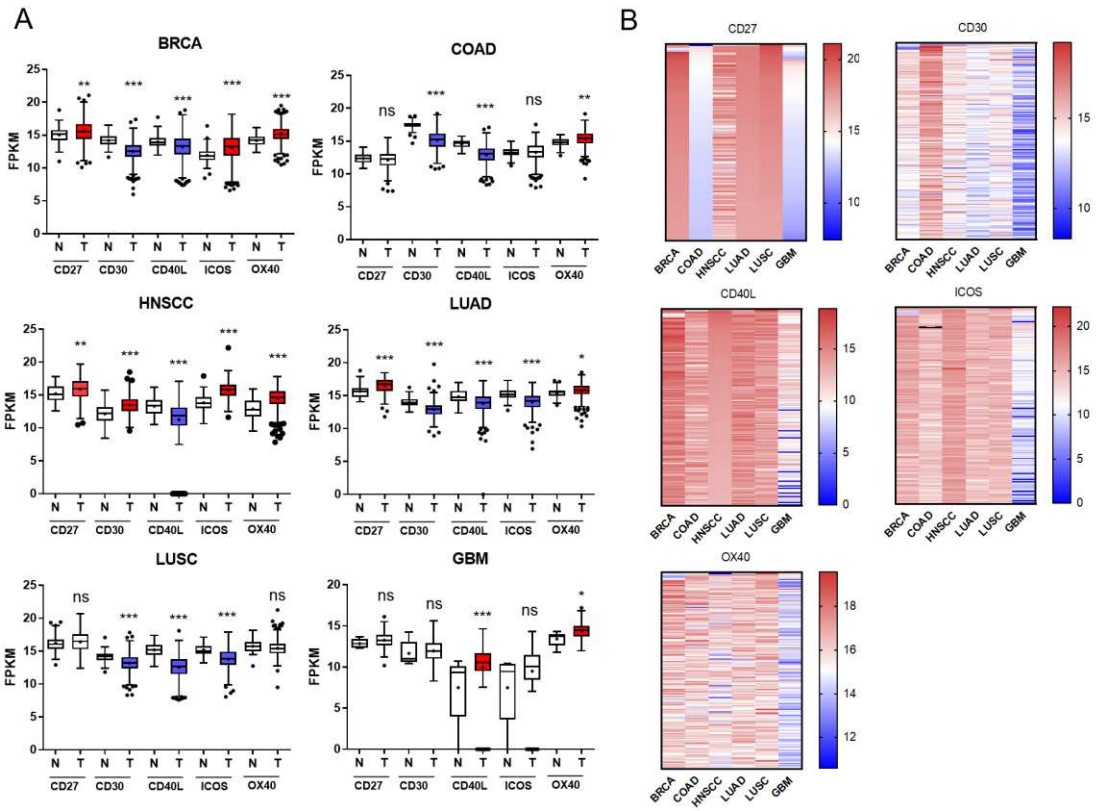

Fig,4. The expression of ICSs in major malignancies of breast, colon, lung, and brain in addition to HNSCC in TCGA dataset. (A) Box and Whisker's plots. The expression of ICSs in normal and tumor tissues in six TCGA cancer datasets. Y axis, FPKM; N, normal tissue; T, tumor tissue. +, medium value; Red box, upregulation; blue box, downregulation; white box, ns. *ns*, not significant. *, ** and *** represent $p < 0.05$, $p < 0.01$ and $p < 0.001$, respectively. *t*-test. (B) Heatmaps illustrating the FPKM of ICSs for individual tumors. Gradient bars delineate the FPKM for each ICS.

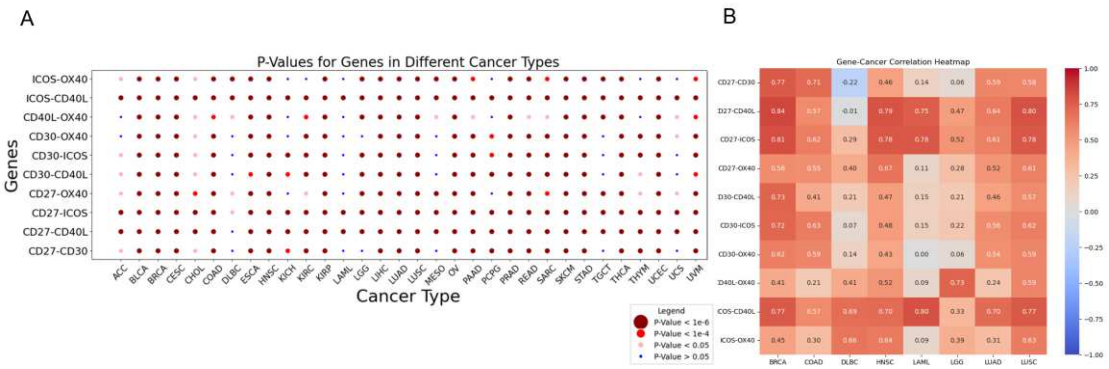

Fig. 5. The pair-wise correlation analysis across ICSs in the TCGA pan-cancer dataset. (A) bubble plot illustrating the significance level of *p* values in pairs across ICSs (Y-axis) and 32 tumor types (X-axis). (B) Heatmap illustrating the r values in pairs across ICSs (Y-axis) and major tumor types (X-axis). The correlation profiles of DLBC and LAML are deviated from other tumors.

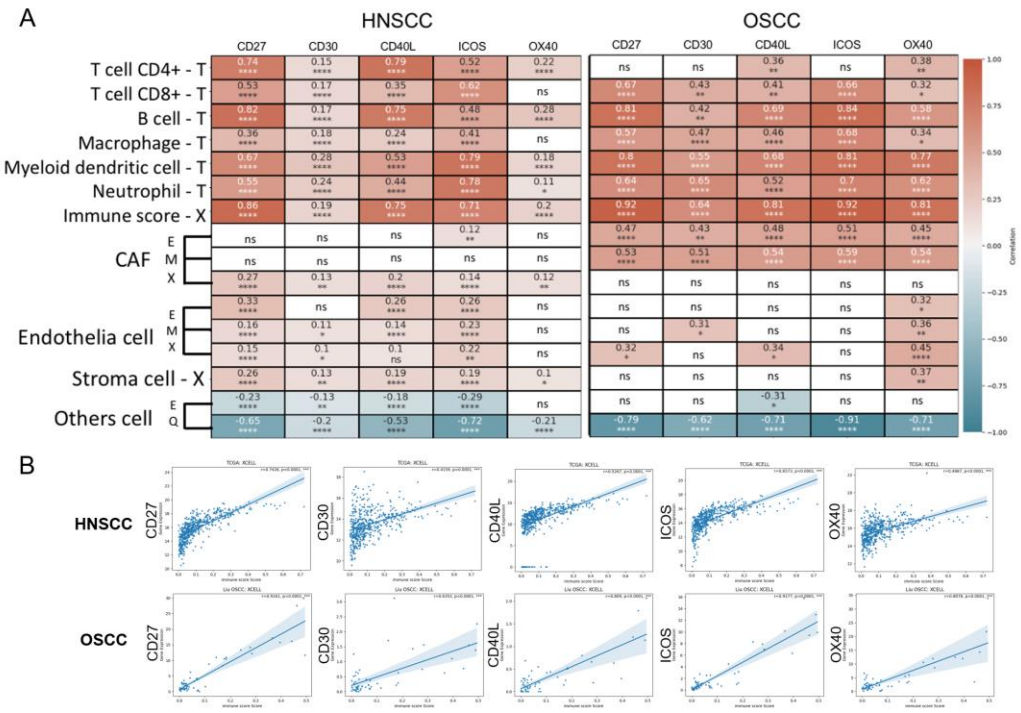

Fig. 6. The immune cell profiles in HNSCC/OSCC. (A) Heatmaps illustrate the correlation between the scores of immune cells and ICSs. Lt, HNSCC. Rt. OSCC. Y-axis, cell type, Abbreviations, the analytical algorithms, Number and gradient bar, *r* value; star sign, *p*-value; E, EPIC, M, MCPCOUNT; Q, QUANTISEQ; T, TIMER; X, XCELL. CAF, cancer-associated fibroblast. *, ** and **** represent $p < 0.05$, $p < 0.001$ and $p < 0.0001$, respectively. Other cells are most likely tumor cells. (B) Individual correlation analysis. Upper, HNSCC; Lower, OSCC; Y-axis, ICSs; X-axis, immune score revealed by XCELL program; line, correlation line; blue zone, 95% confidence interval.

Supplementary Files

This is a list of supplementary files associated with this preprint. Click to download.

- 2024ICSsupplements.BMCOH..docx